A finite element model using a unified formulation for the analysis of viscoelastic sandwich laminates.

A finite element model using a unified formulation for the analysis of viscoelastic sandwich laminates

A. J. M. Ferreira [a], A.L. Araújo [b] A. M. A. Neves [c], J. D. Rodrigues [d], E. Carrera [e], M. Cinefra [e], C. M. Mota Soares [b]

[a] *(Corresponding author: ferreira@fe.up.pt) Departamento de Engenharia Mecânica, Faculdade de Engenharia, Universidade do Porto, Rua Dr. Roberto Frias, 4200-465 Porto, Portugal*

[b] *IDMEC/IST, Universidade Técnica de Lisboa, Av. Rovisco Pais, 1049-001 Lisboa, Portugal*

[c] *Departamento de Engenharia Mecânica, Faculdade de Engenharia, Universidade do Porto, Rua Dr. Roberto Frias, 4200-465 Porto, Portugal*

[d] *INEGI, Faculdade de Engenharia, Universidade do Porto, Rua Dr. Roberto Frias, 4200-465 Porto, Portugal*

[e] *Departament of Aeronautics and Aerospace Engineering, Politecnico di Torino, Corso Duca degli Abruzzi, 24, 10129 Torino, Italy*

Abstract

In this paper we present a layerwise finite element model for the analysis of sandwich laminated plates with a viscoelastic core and laminated anisotropic face layers. The stiffness and mass matrices of the element are obtained by the Carrera's Unified formulation (CUF). The dynamic problem is solved in the frequency domain with viscoelastic frequency-dependent material properties for the core. The dynamic behaviour of the model is compared with solutions found in the literature, including experimental data.

Keywords

A. Plates; A. Layered structures; B. Vibration; C. Finite Element Analysis (FEA).

1 Introduction

Sandwich plates with viscoelastic core are very effective in reducing and controlling vibration response of lightweight and flexible structures, where the soft core is strongly deformed in shear, due to the adjacent stiff layers. The theoretical work on constrained layer damping can be traced to DiTaranto [1] and Mead and Markus [2] for the axial and bending vibration of sandwich beams. Since then, different formulations and techniques have been reported for modelling and predicting the energy dissipation of the viscoelastic core layer in a vibrating passive constrained layer damping structure [3–5]. Other proposed formulations include thickness deformation of the core layer dealing with the cases where only a portion of the base structure receives treatment [6].

Due to the high shear developed inside the core of the sandwich, equivalent single layer plate theories, even those based on higher order deformations, are not adequate to describe the behaviour of these sandwiches, also due to the high deformation discontinuities that arise at the interfaces between the viscoelastic core material and the surrounding elastic constraining layers. The usual approach to analyse the dynamic response of sandwich plates uses a layered scheme of plate and brick elements with nodal linkage. This approach leads to a time consuming spatial modelling task. To overcome these difficulties, the layerwise theory has been considered for constrained viscoelastic treatments, and most recently, Moreira et al. [7,8], among others, presented generalized layerwise formulations in this scope.

More recently, Araújo et al. [9–12] have presented and used for optimisation and viscoelastic material identification purposes a sandwich finite element model based on an eight nodded serendipity plate element. The viscoelastic core layer is modelled according to a higher order shear deformation theory and adjacent elastic and piezoelectric layers are modelled using the first order shear deformation theory. All materials are considered to be orthotropic, with elastic layers being formulated as laminated composite plies. Passive damping is accounted for by using the complex modulus approach, allowing for frequency dependent viscoelastic materials and active damping is incorporated through feedback control laws for co-located control. Also in this framework, Moita et al. [13] developed a simple and efficient non conforming triangular finite element where the viscoelastic core is modelled according to Reissner-Mindlin laminated plate theory and the face layers are modelled according the Kirchhoff-Love plate theory. Another sandwich plate model presented by Moita et al. [14] is based on Reddy's third order shear deformation theory for the core and the face layers are also modelled according to the classical laminated plate theory. These models also contemplate hybrid active-passive damping. A similar model was also presented by Bilasse et al. [15] for non linear vibrations of sandwich plates.

In the present work the stiffness and mass matrices are obtained by the Carrera's Unified Formulation (CUF), firstly proposed in [16–18] for laminated plates and shells and extended to functionally graded (FG) plates in [19–21]. The present formulation considers a displacement-based layerwise formulation, with linear expansion of displacements in each layer, with degrees of freedom u, v, w at each laminate interface.

The dynamic response of the finite element model is validated using a few reference solutions from the literature.

2 Stiffness and Mass matrices by the Unified Formulation

This section intends to detail how the stiffness and mass matrices are obtained, in order to support the relevant (nonlinear) eigenproblem, to be discussed later.

2.1 Geometry and notations for multilayered plates

Consider a laminated plate with N_l layers, where we will denote k for the layer number that starts from the bottom surface. Let x and y be the plate middle surface Ω^k coordinates, where Ω_0 and Ω will also denote the reference surface. Let Γ^k be the layer boundary on Ω^k. Let z and z_k be the plate and layer thickness coordinates; and h, h_k denote plate and layer thickness, respectively. In order to compute integrals in the thickness direction, we also denote A_k as the kth-layer thickness domain. Symbols not affected by k subscript/superscripts refer to the whole plate.

2.2 Displacement assumptions

The present Layerwise (LW) approach considers independent layers, with displacement components $\mathbf{u}$ at each laminate interface. The typical expansion for displacements is expressed as

$$\mathbf{u}^k = F_t \mathbf{u}_t^k + F_b \mathbf{u}_b^k = F_\tau \mathbf{u}_\tau^k; \quad \tau = t, b; k = 1, 2, ..., N_l \tag{1}$$

where t, b denote the top and bottom surfaces of the laminate.We are using linear functions in each layer, as follows:

$$F_b = 0.5 - \frac{1}{h^{(k)}}\left(z - \frac{z_b^{(k)} + z_t^{(k)}}{2}\right); \quad F_t = 0.5 + \frac{1}{h^{(k)}}\left(z - \frac{z_b^{(k)} + z_t^{(k)}}{2}\right) \tag{2}$$

The thickness for each layer is obtained as $h^{(k)} = z_t^{(k)} - z_b^{(k)}$. The quantities referred in equation 2 are illustrated in figure 1 for a 3-layered laminate.

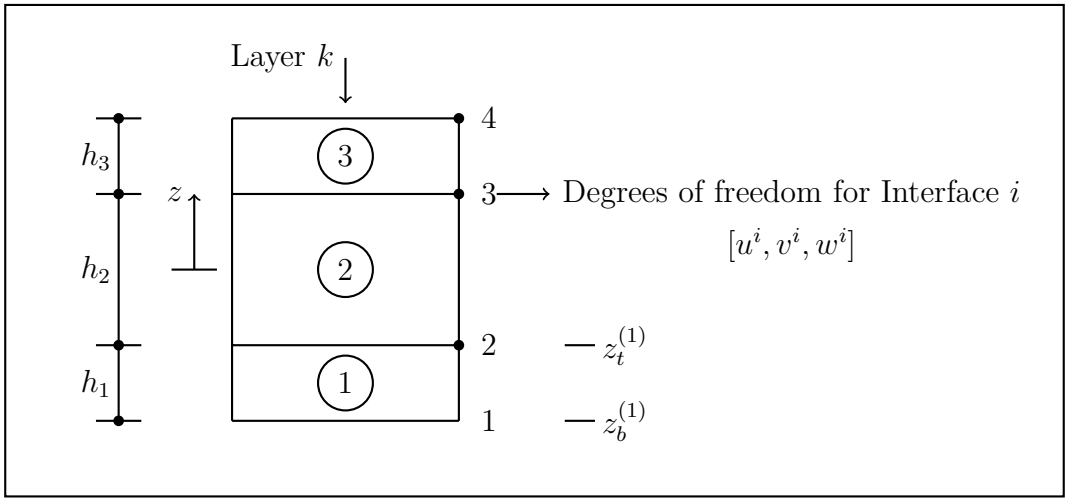

Fig. 1. A 4-layer laminate; definition of degrees of freedom at interfaces

2.3 Strain-displacement relations

Resorting to the small deformation assumptions, the in-plane (p), and out-of-plane (n) strain components $\boldsymbol{\epsilon}_p, \boldsymbol{\epsilon}_n$ are linearly related to the displacements $\boldsymbol{u}$ according to

$$\boldsymbol{\epsilon}_p = \mathbf{D}_p \mathbf{u} \tag{3}$$

$$\boldsymbol{\epsilon}_n = \mathbf{D}_n \mathbf{u} = \left(\mathbf{D}_{n\Omega} + \mathbf{D}_{nz}\right) \mathbf{u} \tag{4}$$

where $\mathbf{u}$ denotes the array of the displacement components,

$$\mathbf{u} = \begin{bmatrix} u_x & u_y & u_z \end{bmatrix}^T \tag{5}$$

The differential matrices are expressed as

$$\mathbf{D}_p = \begin{bmatrix} \frac{\partial}{\partial x} & 0 & 0 \\ 0 & \frac{\partial}{\partial y} & 0 \\ \frac{\partial}{\partial y} & \frac{\partial}{\partial x} & 0 \end{bmatrix}; \mathbf{D}_n = \begin{bmatrix} \frac{\partial}{\partial z} & 0 & \frac{\partial}{\partial x} \\ 0 & \frac{\partial}{\partial z} & \frac{\partial}{\partial y} \\ 0 & 0 & \frac{\partial}{\partial z} \end{bmatrix}; \quad \mathbf{D}_{n\Omega} = \begin{bmatrix} 0 & 0 & \frac{\partial}{\partial x} \\ 0 & 0 & \frac{\partial}{\partial y} \\ 0 & 0 & 0 \end{bmatrix}; \mathbf{D}_{nz} = \begin{bmatrix} \frac{\partial}{\partial z} & 0 & 0 \\ 0 & \frac{\partial}{\partial z} & 0 \\ 0 & 0 & \frac{\partial}{\partial z} \end{bmatrix} \tag{6}$$

2.4 Hooke's law for orthotropic lamina in the material reference system

The linear elastic laminae are considered to be homogeneous. The Hooke's law for the anisotropic k-lamina is written in the form $\sigma_i = C_{ij}\epsilon_j$, where the sub-indices i and j, ranging from 1 to 6, stand for the index couples $11, 22, 33, 13, 23$ and 12, respectively. The material is assumed to be orthotropic. Therefore, $C_{14} = C_{24} = C_{34} = C_{64} = C_{15} = C_{25} = C_{35} = C_{65} = 0$. This implies that σ^k_{13} and σ^k_{23} depend on ϵ^k_{13} and ϵ^k_{23} only. In matrix form it can be written

$$\begin{bmatrix} \sigma_{11} \\ \sigma_{22} \\ \sigma_{12} \\ \sigma_{13} \\ \sigma_{23} \\ \sigma_{33} \end{bmatrix} = \begin{bmatrix} C_{11} & C_{12} & 0 & 0 & 0 & C_{13} \\ C_{12} & C_{22} & 0 & 0 & 0 & C_{23} \\ 0 & 0 & C_{66} & 0 & 0 & 0 \\ 0 & 0 & 0 & C_{55} & 0 & 0 \\ 0 & 0 & 0 & 0 & C_{44} & 0 \\ C_{13} & C_{23} & 0 & 0 & 0 & C_{33} \end{bmatrix} \begin{bmatrix} \epsilon_{11} \\ \epsilon_{22} \\ \epsilon_{12} \\ \epsilon_{13} \\ \epsilon_{23} \\ \epsilon_{33} \end{bmatrix} \tag{7}$$

2.5 Hooke' law for orthotropic lamina in the plate reference system

Multilayered plates are often composed by layers made up with different orientation. It is therefore of interest to write the Hooke's law on the material coordinate system 1,2,3 into the reference coordinate system x, y, z. The relations between the two coordinate systems are expressed as:

$$\boldsymbol{\sigma} = \mathbf{T}\boldsymbol{\sigma_m}; \quad \boldsymbol{\epsilon_m} = \mathbf{T}^{\boldsymbol{T}}\boldsymbol{\epsilon}\ ; \quad \boldsymbol{\sigma_m} = \mathbf{C}\boldsymbol{\epsilon_m} \tag{8}$$

where

$$\boldsymbol{\sigma}_m = \begin{bmatrix} \sigma_{11} & \sigma_{22} & \sigma_{12} & \sigma_{13} & \sigma_{23} & \sigma_{33} \end{bmatrix}^T \tag{9}$$

$$\boldsymbol{\epsilon}_m = \begin{bmatrix} \epsilon_{11} & \epsilon_{22} & \epsilon_{12} & \epsilon_{13} & \epsilon_{23} & \epsilon_{33} \end{bmatrix}^T \tag{10}$$

$$\boldsymbol{\sigma} = \begin{bmatrix} \sigma_{xx} & \sigma_{yy} & \sigma_{xy} & \sigma_{xz} & \sigma_{yz} & \sigma_{zz} \end{bmatrix}^T \tag{11}$$

$$\boldsymbol{\epsilon} = \begin{bmatrix} \epsilon_{xx} & \epsilon_{yy} & \epsilon_{xy} & \epsilon_{xz} & \epsilon_{yz} & \epsilon_{zz} \end{bmatrix}^T \tag{12}$$

and $\mathbf{T}$ denotes the matrix of direction cosines of the coordinate transformation. Using previous relations, we can finally obtain the stress-strain relations in the reference coordinate system as

$$\boldsymbol{\sigma} = \mathbf{T}\mathbf{C}\mathbf{T}^T\boldsymbol{\epsilon} = \tilde{\mathbf{C}}\boldsymbol{\epsilon} \tag{13}$$

2.6 Viscoelastic core

For the viscoelastic core layer, the stiffness coefficients C_{ij} are complex quantities. The complex modulus approach was used in this work, according to the elastic-viscoelastic correspondence principle. In this case, the usual engineering moduli may be represented by complex quantities, considering isothermal conditions (see Araujo et al. [11] for details), as

$$\begin{aligned}
E_1^*(j\omega) &= E_1(\omega)(1 + j\eta_{E_1}(\omega)) \\
E_2^*(j\omega) &= E_2(\omega)(1 + j\eta_{E_2}(\omega)) \\
E_3^*(j\omega) &= E_3(\omega)(1 + j\eta_{E_3}(\omega)) \\
G_{12}^*(j\omega) &= G_{12}(\omega)(1 + j\eta_{G_{12}}(\omega)) \\
G_{23}^*(j\omega) &= G_{23}(\omega)(1 + j\eta_{G_{23}}(\omega)) \\
G_{13}^*(j\omega) &= G_{13}(\omega)(1 + j\eta_{G_{13}}(\omega)) \\
\nu_{12}^*(j\omega) &= \nu_{12}(\omega)(1 - j\eta_{\nu_{12}}(\omega)) \\
\nu_{13}^*(j\omega) &= \nu_{13}(\omega)(1 - j\eta_{\nu_{13}}(\omega)) \\
\nu_{23}^*(j\omega) &= \nu_{23}(\omega)(1 - j\eta_{\nu_{23}}(\omega))
\end{aligned} \tag{14}$$

where E_1, E_2, E_3, G_{12}, G_{23}, G_{13} and ν_{12}, ν_{13}, ν_{23} denote storage moduli, η_{E_1}, η_{E_2}, η_{E_3}, $\eta_{G_{12}}$, $\eta_{G_{23}}$, $\eta_{G_{13}}$ and $\eta_{\nu_{12}}$, $\eta_{\nu_{13}}$, $\eta_{\nu_{23}}$ are the corresponding material loss factors, ω represents the angular frequency of vibration and $j = \sqrt{-1}$ is the imaginary unit.

2.7 Finite element interpolations

Following standard finite element method (FEM) approximations, the unknown variables in the element domain are expressed in terms of their values at the element nodes. According to the isoparametric description, displacements are expressed as

$$\mathbf{u}_\tau^k = N_i \mathbf{q}_{\tau i}^k \ (i = 1, 2, ..., N_n) \tag{15}$$

where

$$\mathbf{q}_{\tau i}^k = \begin{bmatrix} q_{u_x \tau i}^k & q_{u_y \tau i}^k & q_{u_z \tau i}^k \end{bmatrix}^T \tag{16}$$

Here, N_n is the number of element nodes, N_i are the shape functions and $\mathbf{q}_{\tau i}^k$ are nodal variables. Also here ξ, η are the natural coordinates.

The assumed displacemnt field is first introduced in the expression for the strains, leading to the following expressions,

$$\boldsymbol{\varepsilon}_p^k = \mathbf{D}_p \mathbf{u}^k = \mathbf{D}_p \left(F_\tau \mathbf{u}_\tau^k \right) \tag{17}$$

$$\boldsymbol{\varepsilon}_n^k = \mathbf{D}_n \mathbf{u}^k = \left(\mathbf{D}_{n\Omega} + \mathbf{D}_{nz} \right) \left(F_\tau \mathbf{u}_\tau^k \right) = \mathbf{D}_{n\Omega} \left(F_\tau \mathbf{u}_\tau^k \right) + F_{\tau,z} \mathbf{u}_\tau^k \tag{18}$$

In which the notation $F_{\tau,z} = \frac{\partial F_\tau}{\partial z}$ has been introduced. Being the base functions F_τ independent of x and y, the strains can now be written as

$$\boldsymbol{\varepsilon}_p^k = F_\tau \mathbf{D}_p \left(N_i \mathbf{I} \right) \mathbf{q}_{\tau i}^k \; ; \quad \boldsymbol{\varepsilon}_n^k = F_\tau \mathbf{D}_{n\Omega} \left(N_i \mathbf{I} \right) \mathbf{q}_{\tau i}^k + F_{\tau,z} N_i \mathbf{q}_{\tau i}^k \tag{19}$$

in which $\mathbf{I}$ is the identity matrix. By introducing the strain–displacement relations along with the Hooke's law, the internal virtual strain energy can be expressed via the Principle of Virtual Displacements (PVD) statement as

$$\begin{aligned}
\delta L_{int}^k = & \int_\Omega \delta \mathbf{q}_{\tau i}^{kT} \mathbf{D}_p^T \left(N_i \mathbf{I} \right) \tilde{\mathbf{C}}_{pp}^k \left[\int_{A_k} \left(F_\tau F_s \right) dz \right] \mathbf{D}_p \left(N_j \mathbf{I} \right) \mathbf{q}_{sj}^k d\Omega + \\
& + \int_\Omega \delta \mathbf{q}_{\tau i}^{kT} \mathbf{D}_p^T \left(N_i \mathbf{I} \right) \tilde{\mathbf{C}}_{pn}^k \left[\int_{A_k} \left(F_\tau F_s \right) dz \right] \mathbf{D}_{n\Omega} \left(N_j \mathbf{I} \right) \mathbf{q}_{sj}^k d\Omega + \\
& + \int_\Omega \delta \mathbf{q}_{\tau i}^{kT} \mathbf{D}_p^T \left(N_i \mathbf{I} \right) \tilde{\mathbf{C}}_{pn}^k \left[\int_{A_k} \left(F_\tau F_{s,z} \right) dz \right] N_j \mathbf{q}_{sj}^k d\Omega + \\
& + \int_\Omega \delta \mathbf{q}_{\tau i}^{kT} \mathbf{D}_{n\Omega}^T \left(N_i \mathbf{I} \right) \tilde{\mathbf{C}}_{np}^k \left[\int_{A_k} \left(F_\tau F_s \right) dz \right] \mathbf{D}_p \left(N_j \mathbf{I} \right) \mathbf{q}_{sj}^k d\Omega + \\
& + \int_\Omega \delta \mathbf{q}_{\tau i}^{kT} \mathbf{D}_{n\Omega}^T \left(N_i \mathbf{I} \right) \tilde{\mathbf{C}}_{nn}^k \left[\int_{A_k} \left(F_\tau F_s \right) dz \right] \mathbf{D}_{n\Omega} \left(N_j \mathbf{I} \right) \mathbf{q}_{sj}^k d\Omega + \\
& + \int_\Omega \delta \mathbf{q}_{\tau i}^{kT} \mathbf{D}_{n\Omega}^T \left(N_i \mathbf{I} \right) \tilde{\mathbf{C}}_{nn}^k \left[\int_{A_k} \left(F_\tau F_{s,z} \right) dz \right] N_j \mathbf{q}_{sj}^k d\Omega + \\
& + \int_\Omega \delta \mathbf{q}_{\tau i}^{kT} N_i \tilde{\mathbf{C}}_{np}^k \left[\int_{A_k} \left(F_{\tau,z} F_s \right) dz \right] \mathbf{D}_p \left(N_j \mathbf{I} \right) \mathbf{q}_{sj}^k d\Omega + \\
& + \int_\Omega \delta \mathbf{q}_{\tau i}^{kT} N_i \tilde{\mathbf{C}}_{nn}^k \left[\int_{A_k} \left(F_{\tau,z} F_s \right) dz \right] \mathbf{D}_{n\Omega} \left(N_j \mathbf{I} \right) \mathbf{q}_{sj}^k d\Omega + \\
& + \int_\Omega \delta \mathbf{q}_{\tau i}^{kT} N_i \tilde{\mathbf{C}}_{nn}^k \left[\int_{A_k} \left(F_{\tau,z} F_{s,z} \right) dz \right] N_j \mathbf{q}_{sj}^k d\Omega
\end{aligned} \tag{20}$$

where Ω represents the domain of the finite element. To notice one again that subscripts s and j have been used for the finite values of unknown variables while subscripts τ and i have been introduced for their variations. As usual

in two dimensional analysis, the integration in the thickness direction can be made beforehand by introducing the following layer integrals

$$\left(\tilde{\mathbf{Z}}_{pp}^{k\tau s},\ \tilde{\mathbf{Z}}_{pn}^{k\tau s},\ \tilde{\mathbf{Z}}_{np}^{k\tau s},\ \tilde{\mathbf{Z}}_{nn}^{k\tau s},\ \right) = \left(\tilde{\mathbf{C}}_{pp}^{k},\ \tilde{\mathbf{C}}_{pn}^{k},\ \tilde{\mathbf{C}}_{np}^{k},\ \tilde{\mathbf{C}}_{nn}^{k}\right) E_{\tau s} \tag{21}$$

$$\left(\tilde{\mathbf{Z}}_{pn}^{k\tau s_{,z}},\ \tilde{\mathbf{Z}}_{nn}^{k\tau s_{,z}},\ \tilde{\mathbf{Z}}_{np}^{k\tau_{,z} s},\ \tilde{\mathbf{Z}}_{nn}^{k\tau_{,z} s_{,z}}\right) = \left(\tilde{\mathbf{C}}_{pn}^{k} E_{\tau s_{,z}},\ \tilde{\mathbf{C}}_{nn}^{k} E_{\tau s_{,z}},\ \tilde{\mathbf{C}}_{np}^{k} E_{\tau_{,z} s},\ \tilde{\mathbf{C}}_{nn}^{k} E_{\tau_{,z} s},\ \tilde{\mathbf{C}}_{nn}^{k} E_{\tau_{,z} s_{,z}}\right) \tag{22}$$

where

$$\left(E_{\tau s},\ E_{\tau s_{,z}},\ E_{\tau_{,z} s},\ E_{\tau_{,z} s_{,z}}\right) = \int_{A_k} \left(F_\tau F_s,\ F_\tau F_{s_{,z}},\ F_{\tau_{,z}} F_s,\ F_{\tau_{,z}} F_{s_{,z}}\right) dz \tag{23}$$

Note that F_τ, F_s have been introduced before for each layer as F_b, F_t in equation 2.

Eqn.(20) can be written as

$$\delta L_{int}^{k} = \delta \mathbf{q}_{\tau i}^{kT} \mathbf{K}^{k\tau sij} \mathbf{q}_{sj}^{k} \tag{24}$$

where $\mathbf{K}^{k\tau sij}$ represents the k-th layer stiffness matrix, defined as

$$\begin{aligned}
\mathbf{K}^{k\tau sij} = {} & \triangleleft \mathbf{D}_p^T \left(N_i \mathbf{I}\right) \left[\tilde{\mathbf{Z}}_{pp}^{k\tau s} \mathbf{D}_p \left(N_j \mathbf{I}\right) + \tilde{\mathbf{Z}}_{pn}^{k\tau s} \mathbf{D}_{n\Omega} \left(N_j \mathbf{I}\right) + \tilde{\mathbf{Z}}_{pn}^{k\tau s_{,z}} N_j\right] + \\
& + \mathbf{D}_{n\Omega}^T \left(N_i \mathbf{I}\right) \left[\tilde{\mathbf{Z}}_{np}^{k\tau s} \mathbf{D}_p \left(N_j \mathbf{I}\right) + \tilde{\mathbf{Z}}_{nn}^{k\tau s} \mathbf{D}_{n\Omega} \left(N_j \mathbf{I}\right) + \tilde{\mathbf{Z}}_{nn}^{k\tau s_{,z}} N_j\right] + \\
& + N_i \left[\tilde{\mathbf{Z}}_{np}^{k\tau_{,z} s} \mathbf{D}_p \left(N_j \mathbf{I}\right) + \tilde{\mathbf{Z}}_{nn}^{k\tau_{,z} s} \mathbf{D}_{n\Omega} \left(N_j \mathbf{I}\right) + \tilde{\mathbf{Z}}_{nn}^{k\tau_{,z} s_{,z}} N_j\right] \triangleright_\Omega
\end{aligned} \tag{25}$$

The symbols $\triangleleft \ldots \triangleright_\Omega$ denote integrals on the finite element domain, Ω.
To notice that the matrix $\mathbf{K}^{k\tau sij}$ is made by triplicate products of 3×3 arrays, so that $\mathbf{K}^{k\tau sij}$ is itself a 3×3 array. Such an array consist of the fundamental nucleus of finite element matrices related to PVD applications. The 9 terms

for $\mathbf{K}^{k\tau sij}$ can be explicitly presented as:

$$
\begin{aligned}
K_{xx}^{k\tau sij} &= \tilde{Z}_{pp11}^{k\tau s} \lhd N_{i,x}N_{j,x} \rhd_\Omega + \tilde{Z}_{pp16}^{k\tau s} \lhd N_{i,y}N_{j,x} \rhd_\Omega + \tilde{Z}_{pp16}^{k\tau s} \lhd N_{i,x}N_{j,y} \rhd_\Omega + \\
&+ \tilde{Z}_{pp66}^{k\tau s} \lhd N_{i,y}N_{j,y} \rhd_\Omega + \tilde{Z}_{nn55}^{k\tau,zs,z} \lhd N_i N_j \rhd_\Omega \\
\\
K_{xy}^{k\tau sij} &= \tilde{Z}_{pp12}^{k\tau s} \lhd N_{i,x}N_{j,y} \rhd_\Omega + \tilde{Z}_{pp26}^{k\tau s} \lhd N_{i,y}N_{j,y} \rhd_\Omega + \tilde{Z}_{pp16}^{k\tau s} \lhd N_{i,x}N_{j,x} \rhd_\Omega + \\
&+ \tilde{Z}_{pp66}^{k\tau s} \lhd N_{i,y}N_{j,x} \rhd_\Omega + \tilde{Z}_{nn45}^{k\tau,zs,z} \lhd N_i N_j \rhd_\Omega \\
\\
K_{xz}^{k\tau sij} &= \tilde{Z}_{pn13}^{k\tau s,z} \lhd N_{i,x}N_j \rhd_\Omega + \tilde{Z}_{pn36}^{k\tau s,z} \lhd N_{i,y}N_j \rhd_\Omega + \tilde{Z}_{nn55}^{k\tau,zs} \lhd N_i N_{j,x} \rhd_\Omega + \\
&+ \tilde{Z}_{nn45}^{k\tau,zs} \lhd N_i N_{j,y} \rhd_\Omega \\
\\
K_{yx}^{k\tau sij} &= \tilde{Z}_{pp12}^{k\tau s} \lhd N_{i,y}N_{j,x} \rhd_\Omega + \tilde{Z}_{pp16}^{k\tau s} \lhd N_{i,x}N_{j,x} \rhd_\Omega + \tilde{Z}_{pp26}^{k\tau s} \lhd N_{i,y}N_{j,y} \rhd_\Omega + \\
&+ \tilde{Z}_{pp66}^{k\tau s} \lhd N_{i,x}N_{j,y} \rhd_\Omega + \tilde{Z}_{nn45}^{k\tau,zs,z} \lhd N_i N_j \rhd_\Omega \\
\\
K_{yy}^{k\tau sij} &= \tilde{Z}_{pp22}^{k\tau s} \lhd N_{i,y}N_{j,y} \rhd_\Omega + \tilde{Z}_{pp26}^{k\tau s} \lhd N_{i,x}N_{j,y} \rhd_\Omega + \tilde{Z}_{pp26}^{k\tau s} \lhd N_{i,y}N_{j,x} \rhd_\Omega + \\
&+ \tilde{Z}_{pp66}^{k\tau s} \lhd N_{i,x}N_{j,x} \rhd_\Omega + \tilde{Z}_{nn44}^{k\tau,zs,z} \lhd N_i N_j \rhd_\Omega \\
\\
K_{yz}^{k\tau sij} &= \tilde{Z}_{pn23}^{k\tau s,z} \lhd N_{i,y}N_j \rhd_\Omega + \tilde{Z}_{pn36}^{k\tau s,z} \lhd N_{i,x}N_j \rhd_\Omega + \tilde{Z}_{nn45}^{k\tau,zs} \lhd N_i N_{j,x} \rhd_\Omega + \\
&+ \tilde{Z}_{nn44}^{k\tau,zs} \lhd N_i N_{j,y} \rhd_\Omega \\
\\
K_{zx}^{k\tau sij} &= \tilde{Z}_{nn55}^{k\tau s,zk} \lhd N_{i,x}N_j \rhd_\Omega + \tilde{Z}_{nn45}^{k\tau s,zk} \lhd N_{i,y}N_j \rhd_\Omega + \tilde{Z}_{np13}^{k\tau,zs} \lhd N_i N_{j,x} \rhd_\Omega + \\
&+ \tilde{Z}_{np36}^{k\tau,zs} \lhd N_i N_{j,y} \rhd_\Omega \\
\\
K_{zy}^{k\tau sij} &= \tilde{Z}_{nn45}^{k\tau s,zk} \lhd N_{i,x}N_j \rhd_\Omega + \tilde{Z}_{nn44}^{k\tau s,zk} \lhd N_{i,y}N_j \rhd_\Omega + \tilde{Z}_{np23}^{k\tau,zs} \lhd N_i N_{j,y} \rhd_\Omega + \\
&+ \tilde{Z}_{np36}^{k\tau,zs} \lhd N_i N_{j,x} \rhd_\Omega \\
\\
K_{zz}^{k\tau sij} &= \tilde{Z}_{nn55}^{k\tau sk} \lhd N_{i,x}N_{j,x} \rhd_\Omega + \tilde{Z}_{nn45}^{k\tau sk} \lhd N_{i,y}N_{j,x} \rhd_\Omega + \tilde{Z}_{nn45}^{k\tau sk} \lhd N_{i,x}N_{j,y} \rhd_\Omega + \\
&+ \tilde{Z}_{nn44}^{k\tau sk} \lhd N_{i,y}N_{j,y} \rhd_\Omega + \tilde{Z}_{nn33}^{k\tau,zs,z} \lhd N_i N_j \rhd_\Omega
\end{aligned}
\tag{26}
$$

The adequate choice of shape functions N, element number of nodes N_n, and the expansion vector $F^{(k)} = [F_b^{(k)}, F_t^{(k)}]$, allows the computation of the stiffness (and mass) matrices of the k-th layer, corresponding to any two-dimensional

theory.

3 Equations of motion

The equations of motion for the plate are obtained by applying the extended Hamilton's principle, using a nine node Lagrangian plate element with 12 mechanical degrees of freedom per node (3 displacements $\times$ 4 interfaces)

$$\mathbf{M}\ddot{\mathbf{u}} + \mathbf{K}(\omega)\mathbf{u} = \mathbf{f} \tag{27}$$

where $\mathbf{u}$, and $\ddot{\mathbf{u}}$, are displacement degrees of freedom and corresponding accelerations, respectively. $\mathbf{M}$ and $\mathbf{K}(\omega)$ are the real mass matrix and complex frequency dependent stiffness matrix, respectively, and $\mathbf{f}$ is the externally applied load vector.

Assuming harmonic vibrations, the final equilibrium equations are given in the frequency domain by:

$$\left[\mathbf{K}(\omega) - \omega^2\mathbf{M}\right]\mathbf{U} = \mathbf{F} \tag{28}$$

where $\mathbf{F}(\omega) = \mathcal{F}(\mathbf{f}(t))$ is the Fourier transform of the time domain force history $\mathbf{f}(t)$ and $\mathbf{U}(\omega) = \mathcal{F}(\mathbf{u}(t))$ is the Fourier transform of the time domain displacement vector $\mathbf{u}(t)$

For the free vibration problem the equations of motion reduce to the following non-linear eigenvalue problem due to the frequency dependent nature of the stiffness matrix:

$$\left[\mathbf{K}(\omega) - \lambda_n^*\mathbf{M}\right]\mathbf{U}_n = \mathbf{0} \tag{29}$$

where $\mathbf{U}_n$ is a complex eigenvector and λ_n^* is the associated complex eigenvalue, which can be written as:

$$\lambda_n^* = \lambda_n\left(1 + j\eta_n\right) \tag{30}$$

and $\lambda_n = \omega_n^2$ is the real part of the complex eigenvalue and η_n is the corresponding modal loss factor.

The non-linear eigenvalue problem is solved iteratively, and the iterative process is considered to have converged when:

$$\frac{\|\omega_i - \omega_{i-1}\|}{\omega_{i-1}} \leq \epsilon \tag{31}$$

where ω_i and ω_{i-1} are current and previous iteration values for the real part of the particular eigenfrequency of interest, respectively, and ϵ is the convergence tolerance.

According to CUF [16–18], the mass matrix (independent of the frequency) components are explicitly obtained as

$$\begin{aligned}
M_{11}^{k\tau sij} =& m_{\tau s}^{k} \lhd N_i N_j \rhd_\Omega \\
M_{12}^{k\tau sij} =& 0 \\
M_{13}^{k\tau sij} =& 0 \\
M_{21}^{k\tau sij} =& 0 \\
M_{22}^{k\tau sij} =& m_{\tau s}^{k} \lhd N_i N_j \rhd_\Omega \\
M_{23}^{k\tau sij} =& 0 \\
M_{31}^{k\tau sij} =& 0 \\
M_{32}^{k\tau sij} =& 0 \\
M_{33}^{k\tau sij} =& m_{\tau s}^{k} \lhd N_i N_j \rhd_\Omega
\end{aligned} \tag{32}$$

where

$$m_{\tau s}^{k} = \int_{A_k} \rho^k F_\tau F_s \, dz$$

4 Applications

In this paper we present comparative results for natural frequencies and modal loss factors with reference numerical and experimental results.

4.1 Sandwich plates

4.1.1 Undamped sandwich

A symmetric and simply supported rectangular sandwich plate with aluminium face layers and a soft orthotropic core is considered [26,28]. The plate in-plane dimensions ($a \times b$) are 1.829 m $\times$ 1.219 m, the thickness for the face layers are 0.406×10^{-3} m, and for the core is 0.635×10^{-2} m. The aluminium

face layers are isotropic with elastic properties $E = 7.023 \times 10^4$ MPa, $\nu = 0.3$ and material density $\rho = 2.82 \times 10^3\,\mathrm{kg/m^3}$. The orthotropic soft core is characterized by the following properties (principal material direction 1 is aligned with the x direction): $E_1 = E_2 = 137$ MPa, $G_{12} = 45.7$ MPa, $G_{13} = 137$ MPa, $G_{23} = 52.7$ MPa, $\nu_{12} = 0.5$, and $\rho = 124.1\,\mathrm{kg/m^3}$.

We compare the present results with FEM analysis by Araujo et al. [11], that employed Serendipity elements, using a Mindlin-like theory for the faces, and a higher-order approach for the core. We also compare with 3-node FEM results by Rikards et al. [26], and experimental results from [28], as reported in [26]. Comparative results for the first ten natural frequencies are presented in table 1, using various Q9 meshes. A very good agreement can be observed between the present numerical results and the reference numerical and experimental ones.

4.1.2 Damped sandwich

A non-symmetric square simply supported sandwich plate with a thick damped core is considered [26,29]. The material properties and geometry of the plate are characterized by non-dimensional quantities. The plate in-plane dimensions are $(a \times a)$ with $a = 100$, the thickness of the face layers are 0.4 and 0.28, and the thickness of the core layer is 4. The face layers are isotropic with elastic properties $E = 10^5$, $\nu = 0.3$ and material density $\rho = 1$. The isotropic soft core is characterized by the following non-dimensional properties: $G = 1$, $\nu = 0.3$, $\rho = 0.5$, and $\eta_G = 0.5$ (material loss factor associated with shear modulus).

We compare the present results with FEM analysis by Araujo et al. [11], that employed Serendipity elements, using a Mindlin-like theory for the faces, and a higher-order approach for the core. We also compare with FEM results by Rikards et al. [26], and Sadasiva and Nakra [29]. Comparative results for the first three modal loss factors and frequencies are presented in tables 2 and 3, respectively, using various Q9 meshes for both present and reported [26,29] results, where a good agreement can be observed. The approximate nature of the energy method used by Rikards et al. [26] to calculate the modal loss factor might explain the deviations observed.

4.2 Sandwich beam

We consider now a clamped-free sandwich beam example from Barkanov et al. [27]. The beam has dimensions: width=0.05m, length=0.3m, and thickness of layers: h_1=0.0012m, h_2=0.0001016m, h_3=0.0008m. The external layers are made out of aluminium 2024T6 with the following properties: E=64GPa,

Table 1
Natural frequencies [Hz] for the undamped rectangular sandwich plate

n	Experimental [28]	FEM [28]	Rikards et al. [26]	Araujo et al. [11]	Present (4×4 Q9)	(8×4 Q9)	(12×10 Q9)
1	–	23	23.4	23.5	23.28	23.27	23.26
2	45	44	45.4	44.8	44.91	44.63	44.60
3	69	69	72.2	71.7	70.93	70.93	70.27
4	78	78	81.6	79.5	83.04	80.09	79.90
5	92	90	95.9	92.5	91.97	91.72	91.08
6	129	123	133.7	126.5	128.90	126.27	125.51
7	133	126	134.2	126.8	139.28	129.83	128.85
8	152	143	152.2	150.7	151.62	151.62	145.16
9	169	162	156.8	170.7	171.56	171.36	165.16
10	177	172	190.9	173.0	181.46	174.74	173.29

Table 2
Modal loss factors for the square damped sandwich plate

Vibration mode m n	FEM [29]	Rikards et al. [26]	Araujo et al. [11]	Present (4×4 Q9)	(8×8 Q9)	(12×12 Q9)
1 1	0.373	0.350	0.368	0.352	0.353	0.353
1 2	0.273	0.173	0.272	0.247	0.248	0.248
1 3	0.189	0.160	0.188	0.160	0.167	0.167

Vibration mode m n	Araujo et al. [11]	Present (4×4 Q9)	(8×8 Q9)	(12×12 Q9)
1 1	0.011	0.0111	0.0111	0.0111
1 2	0.020	0.0211	0.0210	0.0210
1 3	0.034	0.0377	0.0365	0.0364

Table 3
Frequencies (Hz) for the square damped sandwich plate

ν=0.32, and ρ=2695 kg/m^3. The beam is clamped on the left side and free elsewhere. The dynamic characteristics such as its eigenfrequencies and corresponding loss factors have been determined from numerical experiments using a complex eigenvalues method and the following material properties of the 3M damping polymer ISD-112:

$$\begin{aligned} G &= 4.759 - 0.9266/z + 2.405z^2 \quad \text{[MPa]} \\ \text{with} \quad z &= 0.1918 + 0.0005148f \\ \eta_G = \eta_E &= 1.385 - 0.03673z - 0.01342/z \\ \text{with} \quad z &= 0.01 + 0.0006306f \end{aligned}$$

where $f = \frac{\omega}{2\pi}$, and z is not related to thickness coordinate.. Poisson's ratio and density for the viscoelastic core are $\nu = 0.49$ and $\rho = 1000kg/m^3$, respectively.

We use several Q9 meshes to compare frequencies and modal loss factors with results by Barkanov et al. [27]. Because we are modelling a beam, we present two sets of results, one set with Poisson's ratios equal to 0.3, and another set with zero Poisson's ratios. As seen in table 4, the second set presents very close results to those of [27].

4.3 A sandwich plate with frequency-dependent viscoelastic core

A simply supported rectangular sandwich plate of in-plane dimensions 348 mm $\times$ 304.8 mm is made of two face layers with equal thickness of 0.762 mm and a viscoelastic core with a thickness of 0.254 mm. The material of the face layers is isotropic with Young modulus E=68.9 GPa, Poisson's ratio $\nu = 0.3$ and mass density $\rho = 2740$ kg/m^3.

We consider two different materials for the viscoelastic core. The first material is a polymer represented by a constant viscoelastic model with E=2.67008 MPa,

Table 4
Verification of dynamic characteristics for the sandwich beam

Mode n	$f_n^{(exp)}$ [27]	$f_n^{(FEM)}$ [27]	$\eta_n^{(exp)}$ [27]	$\eta_n^{(FEM)}$ [27]	Present $f_n(8 \times 2$ Q9)	η_n	f_n $(10 \times 4$ Q9)	η_n
$\nu_{13} = \nu_{23} = \nu_{12} = 0.3$ for skins								
1	16	16	0.12	0.13	17.0316	0.1095	17.039	0.1092
2	100	99	0.22	0.22	104.4976	0.1848	104.5322	0.1843
3	268	271	0.26	0.25	288.7436	0.2104	288.6668	0.2097
4	496	510	0.26	0.28	496.7389	0.2728	495.2132	0.2725
$\nu_{13} = \nu_{23} = \nu_{12} = 0.0$ for skins								
1	16	16	0.12	0.13	16.4004	0.1179	16.4003	0.1179
2	100	99	0.22	0.22	100.6279	0.1993	100.6161	0.1992
3	268	271	0.26	0.25	277.7424	0.2266	277.4800	0.2265
4	496	510	0.26	0.28	525.4678	0.2644	523.6329	0.2641

$\nu = 0.49$, $\rho = 999$ kg$/m^3$ and constant loss factor $\eta = 0.5$. Results for the first six natural frequencies and modal loss factors are presented in table 5.

The second material is the 3M ISD112 which has a mass density of $\rho = 1600$ kg$/m^3$ and a Poisson's ratio of $\nu = 0.5$, and its shear modulus is frequency dependent and represented by the generalized Maxwell model [30]:

$$G^*(\omega) = G_0 \left(1 + \sum_{i=1}^{n} \frac{\Delta_i \omega}{\omega - j\Omega_i}\right) \tag{33}$$

where G_0 represents the static shear modulus and (Δ_i,Ω_i) the Maxwell parameters obtained by master curves fitting [30].

The 3M ISD112 core is considered at 27 °C. The static shear modulus at this temperature is $G_0 = 0.5 \times 10^6$ Pa [30] and the corresponding Maxwell series terms (Δ_i,Ω_i) involved in the frequency dependent shear modulus are given in table 6. The results for the first four natural frequencies and modal loss factors are presented in table 7 for $\omega = \omega_0$, where ω_0 is the natural frequency obtained considering $\omega = 0$ in equation (29), following [15].

We use several Q9 meshes to compare with results by Trindade et al. [31], that used 3D cores but thin plate faces. For simply-supported (SSSS) plates, the results shown in tables 5 and 7 are excellent. For clamped (CCCC) supports, the results show deviation of 3%. This can perhaps be explained by the fact that our layerwise approach considers 3D theory for every layer, not only for the cores, as in [30].

5 Conclusions

A new sandwich layerwise plate finite element model has been developed via a Unified Formulation for the analysis of the dynamic response of plate structures with passive damping. The complex modulus approach was used for the viscoelastic core material, along with frequency domain response analysis, allowing for frequency dependent material data. The 3D constitutive equations were applied to all laminate layers. The developed nine node finite element model presents a good behaviour with passive damping, when compared to reference solutions. The response of the model has also been compared with experimental data available in the literature, showing excellent agreement.

Table 5
Natural frequencies and associated loss factors corresponding to the first six vibration modes of the sandwich plate with a constant complex core's modulus, core's loss factor $\eta_c = 0.5$ [30]

Trindade et al. [30]		Analytical [31]		Present (4×4 Q9)		8×8 Q9		12×12 Q9	
SSSS									
$\Omega(Hz)$	η_l	$\Omega(Hz)$	η_l	$\Omega(Hz)$	η_l	$\Omega(Hz)$	η_l	$\Omega(Hz)$	η_l
58.0	0.170	60.3	0.190	58.6323	0.1853	58.6094	0.1852	58.6082	0.1852
113.8	0.193	115.4	0.203	112.8628	0.2048	112.2867	0.2049	112.2535	0.2049
129.5	0.192	130.6	0.199	127.8021	0.2016	127.0450	0.2019	127.0013	0.2020
177.2	0.172	178.7	0.181	174.5079	0.1848	173.4775	0.1859	173.4180	0.1860
194.6	0.169	195.7	0.174	195.9840	0.1756	190.1897	0.1793	189.8335	0.1795
232.9	0.156	-	-	233.7982	0.1612	226.1713	0.1655	225.7038	0.1658
CCCC									
87.4	0.189	87.4	0.189	85.1698	0.1923	85.0548	0.1924	85.0505	0.1924
148.9	0.164	148.9	0.165	146.5786	0.1684	144.6418	0.1703	144.5534	0.1704
170.3	0.153	169.9	0.154	167.4410	0.1574	164.8201	0.1599	164.6948	0.1601
223.9	0.139	223.9	0.139	220.6600	0.1427	216.7321	0.1457	216.5612	0.1459
241.1	0.134	241.0	0.134	252.2491	0.1297	233.9649	0.1407	233.1593	0.1413
291.3	0.118	289.8	0.118	305.3447	0.1139	281.0635	0.1253	279.9708	0.1260

6 Acknowledgements

The authors thank the financial support of FCT, through POCTI and POCI(2010) / FEDER. In particular the support of LAETA to project Composites in Mechanical Design and the support to PTDC/EME-PME/120830/2010 is gratefully acknowledged. The authors also acknowledge the kind support of FCT

i	Δ_i	Ω_i (rad/s)
1	0.746	468.7
2	3.265	4742.4
3	43.284	71532.5

Table 6
Maxwell series terms at 27 °C of the 3M ISD112 viscoelastic material [30]

to project PTDC/EME-PME/109116/2008.

References

[1] DiTaranto, R.A. (1965). Theory of vibratory bending for elastic and viscoelastic layered finite-length beams, *ASME Journal of Applied Mechanics*, **32**:881–886.

[2] Mead, D.J. and Markus, S. (1969). The forced vibration of a three-layer, damped sandwich beam with arbitrary boundary conditions, *AIAA Journal*, **10**:163–175.

[3] Rao, D.K. (1978). Frequency and loss factors of sandwich beams under various boundary conditions, *International Journal of Mechanical Engineering Science*, **20**:271–278.

[4] Yan, M.J. and Dowell, E.H. (1972). Governing equations of vibrating constrained-layer damping sandwich plates and beams, *ASME Journal of Applied Mechanics*, **39**:1041–1046.

[5] Rao, M.D. and He, S. (1993). Dynamic analysis and design of laminated composite beams with multiple damping layers, *AIAA Journal*, **31**:736–745.

[6] Douglas, B.E. and Yang, J.C.S. (1978). Transverse compressional damping in the vibratory response of elastic-viscoelastic beams, *AIAA Journal*, **16**:925–930.

[7] Moreira, R.A.S., Rodrigues, J.D., Ferreira, A.J.M. A generalized layerwise finite element for multi-layer damping treatments. Computational Mechanics. 37, 426-444 (2006)

[8] Moreira, R.A.S., Rodrigues, J.D. A layerwise model for thin soft core sandwich plates. Computers and Structures. 84, 1256-1263 (2006)

[9] Araújo, A.L., Mota Soares, C.M., Mota Soares, C.A. Finite element model for hybrid active-passive damping analysis of anisotropic laminated sandwich structures. Journal of Sandwich Structures and Materials. (in press) doi:10.1177/1099636209104534 (2010)

[10] Araújo, A.L., Mota Soares, C.M., Mota Soares, C.A., Herskovits, J. Optimal design and parameter estimation of frequency dependent viscoelastic laminated sandwich composite plates. Composite Structures. 92, 2321-2327 (2010)

[11] Araújo, A.L., Mota Soares, C.M., Mota Soares, C.A. A Viscoelastic Sandwich Finite Element Model for the Analysis of Passive, Active and Hybrid Structures. Applied Composite Materials. 17, 529-542 (2010)

[12] Araújo, A.L., Martins, P., Mota Soares, C.M., Mota Soares, C.A., Herskovits, J. Damping Optimisation of Hybrid Active-Passive Sandwich Composite Structures. Advances in Engineering Software. 46, 69-74 (2012)

[13] Moita, J.S., Araújo, A.L., Martins, P., Mota Soares, C.M., Mota Soares, C.A. A Finite Element Model for the Analysis of Viscoelastic Sandwich Structures. Computers & Structures. 89, 1874-1881 (2011)

[14] Moita, J.S., Araújo, A.L., Martins, P., Mota Soares, C.M., Mota Soares, C.A. Analysis of active-passive plate structures using a simple and efficient finite element model. Mechanics of Advanced Materials and Structures. 18, 159-169 (2011)

[15] Bilasse, M., Azrar, L., Daya, E.M. Complex modes based numerical analysis of viscoelastic sandwich plates vibrations. Computers & Structures. 89, 539-555 (2011)

[16] E. Carrera. Developments, ideas, and evaluations based upon reissner's mixed variational theorem in the modelling of multilayered plates and shells. *Applied Mechanics Reviews*, 54:301–329, 2001.

[17] E. Carrera. Evaluation of layer-wise mixed theories for laminated plate analysis. *AIAA Journal*, (36):830–839, 1998.

[18] Erasmo Carrera. Theories and finite elements for multilayered plates and shells: A unified compact formulation with numerical assessment and benchmarking. *Archives of Computational Methods in Engineering*, 10:215–296.

[19] S. Brischetto and E. Carrera. Advanced mixed theories for bending analysis of functionally graded plates. *Computers and Structures*, 88(23-24):1474 – 1483, 2010.

[20] S. Brischetto. Classical and mixed advanced models for sandwich plates embedding functionally graded cores. *J Mech Mater Struct*, 4:13–33, 2009.

[21] E. Carrera, S. Brischetto, and A. Robaldo. Variable kinematic model for the analysis of functionally graded material plates. *AIAA Journal*, 46:194–203, 2008.

[22] Murakami, H., 1985, Laminated composite plate theory with improved in-plane responses, ASME Proceedings of PVP Conference, New Orleans, June 24-26, PVP-Vol. 98-2, 257-263.

[23] Toledano A, and Murakami H, 1987a, A high-order laminated plate theory with improved in-plane responses, *International Journal of Solids and Structures* , vol 23, pp 111-131.

[24] Toledano A and Murakami H. 1987b, A composite plate theory for arbitrary laminate configurations, *Journal of Applied Mechanics* vol 54 , 181-189.

[25] Carrera E, 1995, A class of two-dimensional theories for anisotropic multilayered plates analysis , *Accademia delle Scienze di Torino*, Memorie Scienze Fisiche, 19-20 (1995-1996), pp 1-39.

[26] Rikards, R., Chate, A., Barkanov, E. Finite element analysis of damping the vibrations of laminated composites. Computers & Structures. 47, 1005-1015 (1993)

[27] Barkanov, E., Skukis, E., Petitjean, B. Characterisation of viscoelastic layers in sandwich panels via an inverse technique, Journal of Sound and Vibration. 327, 402-412 (2009)

[28] Alam, N., Asnani, N.T. Vibration and damping analysis of multilayered rectangular plates with constrained viscoelastic layers. Journal of Sound and Vibration. 97, 597-614 (1984)

[29] Sadasiva Rao, Y.V., Nakra, B.C. Vibrations of unsymmetrical sandwich beams and plates with viscoelastic cores. Journal of Sound and Vibration. 34, 309-326 (1974)

[30] Trindade M, Benjeddou A, Ohayon R. Modeling of frequency dependent viscoelastic materials for active-passive vibration damping. J Vibration Acoust 2000;122(2):169-74.

[31] Johnson C, Kienholz D. Finite element prediction of damping in structures with constrained viscoelastic layers. Am Inst Aeronaut Astronaut J 1982;20:1284Ð90.

[32] Duigou L, Daya EM, Potier-Ferry M. Iterative algorithms for nonlinear eigenvalue problems. Application to vibrations of viscoelastic shells. Comput Methods Appl Mech Eng 2003;192:1323Ð35.

Table 7
Linear vibration characteristics corresponding to the first four vibration modes of the sandwich plate with 3M ISD112 frequency dependent core at 27°C, $\omega \approx \omega_0$ [30]

	[30]			Present (4×4 Q9)			(8×8 Q9)			12×12 Q9		
	$\omega_0(rad/s)$	$\Omega_l(Hz)$	η_l	$\omega_0(rad/s)$	$\Omega_l(Hz)$	η_l	$\omega_0(rad/s)$	$\Omega_l(Hz)$	η_l	$\omega_0(rad/s)$	$\Omega_l(Hz)$	η_l
SSSS	314.84	53.77	0.213	314.0751	53.6872	0.2355	313.9563	53.6659	0.2354	313.9500	53.6648	0.2354
	622.18	110.31	0.272	612.2826	108.4740	0.2909	608.8928	107.8791	0.2908	608.6974	107.8449	0.2908
	712.09	126.72	0.283	697.6239	123.9977	0.2968	693.1220	123.2110	0.2968	692.8626	123.1657	0.2968
	992.11	176.97	0.289	970.4160	172.9414	0.3079	963.7652	171.8744	0.3086	963.3807	171.8128	0.3087
CCCC	481.58	83.01	0.246	467.1247	80.3021	0.2495	466.3763	80.1849	0.2496	466.3443	80.1804	0.2496
	839.07	146.61	0.258	823.2952	143.6186	0.2622	811.0424	141.6222	0.2634	810.4542	141.5311	0.2635
	967.88	168.92	0.257	948.4801	165.2845	0.2607	931.7486	162.5891	0.2625	930.9136	162.4605	0.2627
	1285.48	225.27	0.270	1263.5253	221.0142	0.2733	1238.4071	216.9794	0.2754	1237.2478	216.8068	0.2757